PHYSICAL REVIEW A **73**, 031402(R) (2006)

Dynamic manipulation of Bose-Einstein condensates with a spatial light modulator

V. Boyer,[1] R. M. Godun,[1] G. Smirne,[1] D. Cassettari,[1] C. M. Chandrashekar,[1] A. B. Deb,[1] Z. J. Laczik,[2] and C. J. Foot[1]
[1]*Clarendon Laboratory, University of Oxford, Parks Road, Oxford, OX1 3PU, United Kingdom*
[2]*Department of Engineering Science, University of Oxford, Parks Road, Oxford, OX1 3PJ, United Kingdom*
(Received 23 November 2005; published 31 March 2006)

We manipulate a Bose–Einstein condensate using the optical trap created by the diffraction of a laser beam on a fast ferroelectric liquid crystal spatial light modulator. The modulator acts as a phase grating which can generate arbitrary diffraction patterns and be rapidly reconfigured at rates up to 1 kHz to create smooth, time-varying optical potentials. The flexibility of the device is demonstrated with our experimental results for splitting a Bose–Einstein condensate and independently transporting the separate parts of the atomic cloud.

DOI: 10.1103/PhysRevA.73.031402 PACS number(s): 32.80.Pj, 03.75.Kk, 42.40.My

The miniaturization of atomic traps is key to the use of ultracold atoms in applications requiring full quantum control of the external degrees of freedom, such as quantum information processing or matter wave interferometry. As pointed out in Ref. [1], quantum effects on the propagation of the spatial wave function arise when the trapping potential features details on a length scale smaller than the atomic wavelength, typically 1 μm for ultracold atoms.

One of the two main technologies to realize microtraps is the atom chip [2,3], which consists of microfabricated conducting wires able to generate highly configurable magnetic traps. A common drawback is that the very proximity of the wires or the surface holding the wires ($10-500$ μm) results in undesired perturbations [1,4,5]. Another limitation is that magnetic trapping only works for a subset of all the Zeeman sublevels.

The alternative technology to magnetic atom chips is optical trapping. Atoms in light fields far detuned from atomic resonances can be tightly confined in a nondissipative trap, in any Zeeman sublevel of the ground state [6] and far away from any physical structure. Regular arrangements of microtraps, called optical lattices [7], are obtained by interfering intersecting laser beams. More complex trapping structures have been implemented on cold atoms using microlenses and other micro-optic elements [8,9]. However, compared to the magnetic atom chips, those techniques do not have much flexibility built in, because the shape of the potential is contained in a static optical setup, and only a small number of manipulations can be performed [8].

Programmable diffractive optics can efficiently extend the capabilities of micro-optic components by generating arbitrary light patterns. In colloidal physics experiments using optical tweezers, it is common to generate multiple traps by diffracting the light from spatial light modulators (SLMs) [10]. These programmable diffractive optical elements allow great flexibility and dynamic control of the optical potentials, and dynamic manipulation of plastic beads has been demonstrated [11]. However, before the work reported here, the application of spatial light modulation to move cold atoms had been considered difficult because the motion of atoms is not subject to damping (unlike samples in water), and variation of the potential must be carried out extremely smoothly. Previously, static intensity patterns have been proposed to create hollow guides for cold atoms [12], and have been used to trap atoms in multiple wells [13].

We report the manipulation of a ^{87}Rb Bose–Einstein condensate (BEC) with moving optical tweezers generated by diffraction of a laser beam on the programmable phase grating created by a ferroelectric liquid crystal SLM. We were able to split the BEC into two or three pieces, and to move those pieces in a plane perpendicular to the tweezers. This demonstrates the flexibility of this technique and its ability to create a variety of dynamic optical traps for submicroKelvin atoms.

An SLM is an array of pixels acting as individually tunable absorbers or retardation waveplates which can imprint on a light beam a spatial amplitude modulation or a spatial phase modulation respectively. Common SLMs are made of nematic liquid crystal pixels whose birefringence is controlled by polarizing them with an external electric field. They exhibit a continuous phase retardation effect and a good diffraction efficiency, and were successfully used to create static patterns [13,14]. However, their refresh rate, which is the rate at which the retardation of a pixel can be changed from one value to another, is of the order of 50 Hz, which is too low for most cold atom applications. In order to generate a useful dynamic potential, the device should be able to generate hundreds or thousands of different patterns on the time scale of the experiment, typically a few seconds. For this reason, we used a ferroelectric liquid crystal SLM, which is much faster but is limited to binary values of the retardation, resulting in an imprinted phase of 0 or π [15].

Our device is a 256×256 square-pixel array of total size 4×4 mm from Displaytech, used in reflection. Let x and y be the main axes of the chip. Ferroelectric liquid crystal materials are birefringent, with two bistable orientations for the liquid crystal director. By applying an appropriate electric field, the director can be switched between these two orientations, and the fast axis can be rotated in the xy plane between $\pm22.5°$ with respect to the y axis (Fig. 1). The retardation, which is a function of the thickness of the material, is set to be $\lambda/2$ at $\lambda\simeq700$ nm. As a result, the effect on light linearly polarized along y is a rotation of the polarization through $\pm45°$, depending on the sign of the electric field, and the two possible values of the x component of the polarization of the rotated light are dephased by π. Thus, the x-component of the light reflected from the SLM has a bi-

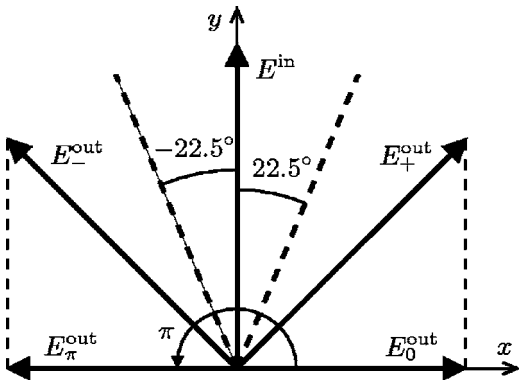

FIG. 1. Polarization effects in a ferroelectric liquid crystal. The electric field E^{in} of the incident light is polarized along the y axis. Depending on the two possible positions of the fast axis (dashed lines), the output polarization $E_\pm^{out}$ is rotated by ±45°. The corresponding possible components along the x axis E_0^{out} and E_π^{out} are dephased with respect to each other by π. The component of the output polarization along the y axis is not dephased and goes into the zeroth order of the diffraction pattern.

nary phase modulation and contributes to the diffraction pattern, whereas the y component of the light is not phase modulated and is reflected into the zeroth order of the diffraction pattern.

We chose to use the diffraction pattern in the far field. Note that the near field can also generate useful trapping potentials, as shown in Refs. [16,17]. In our case, in the scalar approximation, the diffracted electric field is the Fourier transform of the phase pattern on the SLM. There is the same amount of light in the plus and minus first orders, but in practice we only use the plus first order. This, together with the fact that the designed rotation of the incident polarization is 45° instead of 90°, that we use a wavelength for which the retardation effect is less than $\lambda/2$, and that the pixels do not join completely, leads to a diffraction efficiency into the plus first order of only 3%. However, this low efficiency is not of practical importance because only 100 μW are required to trap a BEC in our experimental conditions.

The operation of a ferroelectric SLM presents two kinds of problem. First, in continuous operation, charge migration in the liquid crystal reduces the retardation effect and the light power in the diffraction pattern fades to zero with a time constant of 0.5 s. Charge migration can be prevented by dc balancing the electric field in such a way that the temporal average is close to zero. Thus, the problem is averted when the phase of each pixel is flipped regularly in time. However, the second problem is that the switching of the state of a pixel takes about 250 μs, during which the birefringence is not well defined. Thus, flipping the phase of a large number of pixels at the same time will produce a substantial flicker of the diffraction pattern. Simultaneously solving the dc balancing and the flicker problems requires a compromise between opposite constraints on the level of pixel changes between consecutive filters (phase modulation patterns) of a sequence. Typically, we change less than 10% of the pixels between consecutive filters.

Calculating the filter corresponding to a desired intensity diffraction pattern (target) is a difficult problem in general.

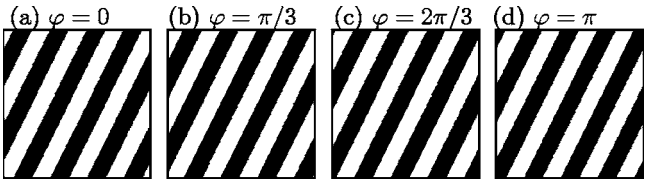

FIG. 2. Four different phase filters realizing the same diffraction pattern consisting of a single spot. The pixels with a zero phase are shown in white and the pixels with a π phase are in black. Each filter has the phase pattern in a different position, corresponding to different phases of the electric field, φ, at the spot position. The filters (a) and (d) are complementary.

The phase of the diffracted field, which is irrelevant to the atoms, is unknown, and assuming a flat phase across the diffraction pattern and taking the reverse Fourier transform of the electric field would give a phase *and* amplitude modulation diffraction grating. In order to obtain a pure phase modulation grating, one has to use algorithms such as an iterative Fourier transform [18], genetic algorithm [19], or direct binary search (DBS) [20]. We use a modified version of DBS [21] which takes care of the flicker and dc balancing issues mentioned above. First, as shown in Ref. [22], the flicker can be reduced by including a term in the DBS error function which keeps account of the pixel changes between consecutive filters. Second, dc balancing requires that *all* the pixels are changed periodically in the sequence, at least a few times per second. We enforce such a change by imposing a time-varying value of the phase of the field at one of the target points with an extra term in the error function. As shown in Fig. 2, modifying the overall phase of the field results in changing the position of the phase pattern on the chip. A small variation of the phase corresponds to the change of a small number of pixels. By carefully setting the weight of the three terms in the error function, we could generate sequences of filters which smoothly moved a set of spots in the Fourier plane, while keeping the flicker below a few percent of the total intensity, and preventing the diffraction pattern from fading away.

To trap cold atoms in the optical potential created by the diffraction pattern of the SLM, we initially create a BEC in a magnetic trap. The BEC apparatus is similar to the one described in Ref. [23], and consists of a pyramidal magneto-optical trap (MOT) feeding a second MOT in a high vacuum glass cell. The atoms are then transfered into a time-averaged orbiting potential [24] and are evaporatively cooled until a BEC containing 2×10^5 atoms is formed. In the final step, the magnetic trap is turned off while the laser beam diffracted by the SLM (2 mm waist on the SLM) is turned on, transfering the atoms into the optical potential. The diffraction pattern is imaged on the trapping zone using the same optics as the absorption imaging system. We thus have access to the atomic distribution in the Fourier plane of the SLM. The smallest spot size waist we can create is $w = 3.8$ μm, slighly larger than the diffraction limit of the optical system. At a wavelength $\lambda = 850$ nm and a power $\mathcal{P} = 0.12$ mW, it creates an optical trap with oscillation frequencies 1.2 kHz radially and 60 Hz in the direction of propagation, and a depth $\epsilon = 2$ μK [25].

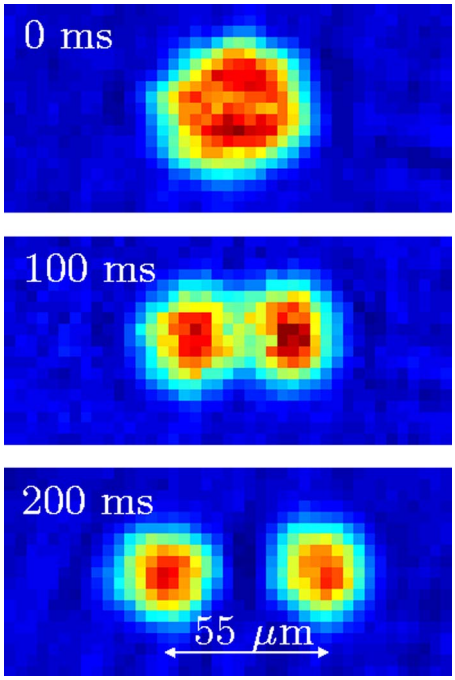

FIG. 3. (Color online) Splitting and transport of a BEC with two optical tweezers. Each frame is an absorption image of the atomic cloud, taken at the time shown on the left.

A BEC of 2×10^5 atoms trapped in such a spot has dimensions of $1.5\ \mu\text{m}\times1.5\ \mu\text{m}\times30\ \mu\text{m}$ and a chemical potential of $0.7\ \mu$K, only one third of the trap depth. This means that very few thermal atoms can be trapped, and the BEC in equilibrium is almost pure. When heating is applied to the cloud, fast evaporation and rethermalization bring the system back to an equilibrium consisting of a quasi-pure BEC with fewer atoms. Because we operate at high peak density, around 10^{15} cm^{-3}, the collision rate is very high and this rethermalization happens on a time scale of a few milliseconds. Unless the heating rate is very high, the cloud stays condensed and the heating translates into atom losses, on top of the other sources of loss. These are dominated by the three-body recombination, which leads to a measured loss rate per atom of $\sim2\ \text{s}^{-1}$ for a BEC of 2×10^5 atoms. We also measure the same losses in an equivalent stationary trap set up without the SLM. This shows that any intensity flicker from the SLM does not translate into a measurable heating rate.

The first of the two experiments that we report here splits the BEC into two parts, as shown in Fig. 3. During 250 ms, the BEC is transfered into a light pattern consisting of two spots in the Fourier plane separated by 6.4 μm [26]. After the magnetic field is switched off, the two spots are moved away from each other until they reach a separation of 55 μm after 200 ms. The refresh rate of the SLM is 500 Hz and the displacement of the spots between each filter is 1/18 of the spot waist. Figure 3 shows the atomic spatial distribution measured by absorption imaging, at various times during the splitting. Each picture represents a different realization of the sequence for which the separation process is interrupted at a given point by turning off the trapping light. The atoms are allowed to free fall for 3 ms before the picture is taken.

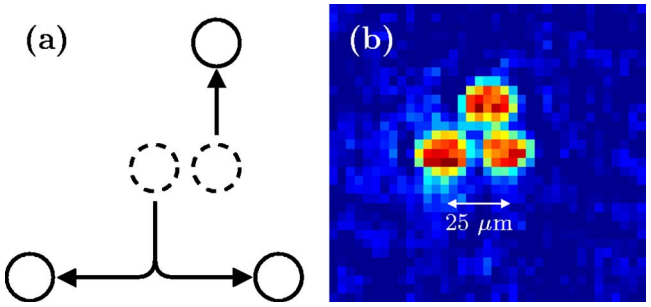

FIG. 4. (Color online) Splitting of a BEC into three pieces. (a) Schematic of the dynamics of the potential, starting from a double-well (dashed lines) to three separate traps (solid lines). (b) Absorption imaging of the BEC in the final trap.

During the imaging process, the atoms are heated up by exchanging photons with a near resonant probe beam, resulting in atomic clouds much more expanded than the original size in the trap. However, the distance between the clouds accurately reflects the separation between the two traps.

In an independent series of experiments, we accurately measure the atom number by allowing the cloud to expand for 15 ms before taking images, and we compare the atom loss of the moving sequence with that of a static double well, which reflects the contribution of three-body recombination only. At the end of the separation sequence shown in Fig. 3, the total atom loss is 50%, half of which is due to the nonadiabatic motion of the potential. The important result is that the nonadiabatic loss reduces to a few percent when using smaller displacements of the spots between consecutive frames of only 1/36 of the spot waist. We find that the splitting generally works well for values of the refresh rate of the SLM ranging from 200 Hz to 1 kHz, but some discrete values have to be avoided in order to prevent strong heating of the BEC; such resonances occur because the refresh rate can have harmonics resonant with the radial oscillation frequency, resulting in a nonadiabatic linear motion which can excite radial oscillations.

To demonstrate further the flexibility of our setup, we load the BEC into a set of three spots in an arrangement that would not be easily achievable using many other techniques. As shown in Fig. 4(a), we start by loading the BEC directly into a double well and, initially, we move the two wells apart vertically until they are separated by 20 μm. We then split the lower spot into two spots which separate horizontally to up to 25 μm. The splitting required careful control of the height and the shape of the potential barrier separating the newly created pair of wells. A picture of the BEC in the final three-spot arrangement is shown in Fig. 4(b). The length of the sequence after the initial loading is 540 ms, and the refresh rate of the SLM is set to 200 Hz. Because we are currently limited to only 128 different filters for technical reasons, we cannot generate a motion of the potential as smooth as the one in the two-spot experiment. As a result, a more severe heating leads to a final number of atoms which is one-half of the number expected when taking into account the three-body recombination only. However, using a larger number of filters would reduce that heating.

In conclusion, we have shown that dynamic optical poten-

tials created with SLMs can be used to manipulate the external degrees of freedom of cold atoms in a controlled manner and with little heating. We believe that combined with high numerical aperture optics, resulting in tightly confining optical tweezers, this versatile technique can play a very important role for applications such as quantum information processing with neutral atoms, where one of the crucial steps is the building of a bus able to carry individual qubits between memory and processing units. Proposals using on-chip magnetic trapping to create quantum processors with mobile qubits can be readily adapted to diffractive optical trapping without having the drawbacks of magnetic trapping. It should be emphasized that the optical traps created by diffraction are not limited to two dimensions and can extend in all directions.

So far, we have focused on dynamic and nontrivial arrangements of spots, but generating other patterns, such as so-called doughnut modes, should be possible, for instance to study persistent currents and superfluid properties.

We acknowledge support from EPSRC, EC (Marie-Curie program, Cold Quantum Gases network), the Royal Society, and DARPA.

[1] Y. J. Lin, I. Teper, C. Chin, and V. Vuletić, Phys. Rev. Lett. **92**, 050404 (2004).
[2] J. Reichel, W. Hänsel, and T. W. Hänsch, Phys. Rev. Lett. **83**, 3398 (1999).
[3] R. Folman, P. Krüger, J. Schmiedmayer, J. Denschlag, and C. Henkel, Adv. At., Mol., Opt. Phys. **48**, 263 (2002).
[4] J. Estève *et al.*, Phys. Rev. A **70**, 043629 (2004).
[5] M. P. A. Jones, C. J. Vale, D. Sahagun, B. V. Hall, and E. A. Hinds, Phys. Rev. Lett. **91**, 080401 (2003).
[6] J. D. Miller, R. A. Cline, and D. J. Heinzen, Phys. Rev. A **47**, R4567 (1993).
[7] J. V. Porto *et al.*, Philos. Trans. R. Soc. London, Ser. A **361**, 1417 (2003).
[8] R. Dumke *et al.*, Phys. Rev. Lett. **89**, 097903 (2002).
[9] R. Dumke, T. Müther, M. Volk, W. Ertmer, and G. Birkl, Phys. Rev. Lett. **89**, 220402 (2002).
[10] D. G. Grier, Nature (London) **424**, 810 (2003).
[11] G. Sinclair *et al.*, Opt. Express **12**, 5475 (2004).
[12] D. McGloin, G. C. Spalding, H. Melville, W. Sibbett, and K. Dholakia, Opt. Express **11**, 158 (2003).
[13] S. Bergamini *et al.*, J. Opt. Soc. Am. B **21**, 1889 (2004).
[14] H. Melville *et al.*, Opt. Express **11**, 3562 (2003).
[15] W. J. Hossack, E. Theofanidou, J. Crain, K. Heggarty, and M. Birch, Opt. Express **11**, 2053 (2003).
[16] R. Newell, J. Sebby, and T. G. Walker, Opt. Lett. **28**, 1266 (2003).
[17] E. Schonbrun *et al.*, Opt. Express **13**, 3777 (2005).
[18] R. W. Gerchberg and W. O. Saxton, Optik (Stuttgart) **35**, 237 (1972).
[19] D. Goldberg, *Genetic Algorithms in Search, Optimization and Machine Learning* (Addison-Wesley, Reading, MA, 1989).
[20] M. A. Seldowitz, J. P. Allebach, and D. W. Sweeney, Appl. Opt. **26**, 2788 (1987).
[21] DBS is an iterative algorithm in which the target is specified by providing the desired intensity level on a finite number of points. The filter is randomly initialized, and the corresponding diffracted intensity (current pattern) is calculated at the target points. An error function provides a measurement of the distance between the current pattern and the target. At each iteration, the phase of a randomly chosen pixel of the filter is flipped if the resulting variation in the error is negative.
[22] V. Boyer, C. M. Chandrashekar, C. J. Foot, and Z. J. Laczik, J. Mod. Opt. **51**, 2235 (2004).
[23] J. Arlt *et al.*, J. Phys. B **32**, 5861 (1999).
[24] W. Petrich, M. H. Anderson, J. R. Ensher, and E. A. Cornell, Phys. Rev. Lett. **74**, 3352 (1995).
[25] The beam propagates horizontally; gravity will reduce the trap depth by about 25%.
[26] Although this distance of 6.4 μm is close to the spot size, the two spots are fully separated. Unlike schemes relying on the incoherent addition of the potentials created by two laser beams, for instance using an acousto-optic modulator with multiple driving frequencies [Y. Shin *et al.*, Phys. Rev. Lett. **92**, 050405 (2004)], the ability to control the light phase at the target allows increased versatility when generating a double well potential. For example, it becomes possible to create two very closely spaced spots which destructively interfere at the mid-point, allowing the spots to be separated by a narrower potential barrier.